

## Trade-offs in thermal and mechanical properties of cellulose films from bacterial cellulose powder induced by ultrasonication duration

Dieter Rahmadiawan<sup>1,2</sup>, Tio Baskara<sup>3</sup>, Hairul Abral<sup>3\*</sup>, Ani Sugiarti<sup>4</sup>, Ahmad Novi Muslimin<sup>4</sup>, Shih-Chen Shi<sup>1</sup>, Thiago F. Santos<sup>5</sup> and Imtiaz Ali Laghari<sup>6</sup>

<sup>1</sup> Department of Mechanical Engineering, National Cheng Kung University, **Taiwan**

<sup>2</sup> Department of Mechanical Engineering, Faculty of Engineering, Universitas Negeri Padang, **Indonesia**

<sup>3</sup> Department of Mechanical Engineering, Faculty of Engineering, Universitas Andalas, **Indonesia**

<sup>4</sup> Research Center for Advanced Materials, National Research and Innovation Agency (BRIN), **Indonesia**

<sup>5</sup> Postgraduate Program in Chemical Engineering, Federal University of Rio Grande do Norte, **Brazil**

<sup>6</sup> Department of Electrical Engineering, The University of Larkano, **Pakistan**

\*Corresponding Author: [abral@eng.unand.ac.id](mailto:abral@eng.unand.ac.id)

*Received:* 06 January 2026; *Revised:* 29 May 2026; *Accepted:* 07 June 2026



Cite this <https://doi.org/10.24036/teknomekanik.v9i2.57372>

**Abstract:** Understanding the trade-offs between thermal and mechanical properties is crucial for optimizing the performance of cellulose films from bacterial cellulose powders (BCP). This study leverages ultrasonication as an eco-friendly method to enhance these properties in BCP-based films while investigating the consequences of varying ultrasonication durations. BCP was sonicated at 250 W for 15 and 30 minutes. Results demonstrated that increasing ultrasonication duration significantly improves tensile strength, toughness, and transparency. The 30-minute sonication yielded the most robust and transparent films, with the highest mechanical strength and toughness. Conversely, while a shorter sonication of 15 minutes slightly improved the thermal stability of the films, increasing  $T_{\max}$  from 317°C for non-sonicated films to 351°C, a longer duration of 30 minutes reduced  $T_{\max}$  to 323°C. This illustrates a clear trade-off between enhancing mechanical properties and maintaining thermal stability. The findings provide insights into a simple yet effective approach for producing environmentally friendly, non-wood-based BC films, emphasizing the need to balance both thermal and mechanical enhancements through controlled ultrasonication.

**Keywords:** bacterial cellulose; cellulose nanocrystal; thermal resistance; ultrasonication duration

### 1. Introduction

The rapid growth of industrial activities, technological development, and global population has led to a substantial increase in energy consumption and resource utilization worldwide. This trend has raised growing concerns regarding environmental pollution, greenhouse gas emissions, and the depletion of finite fossil-based resources [1], [2], [3]. Conventional petroleum-derived materials, which dominate many industrial sectors, often require energy-intensive production processes and generate considerable environmental burdens throughout their life cycle. Consequently, there is an increasing demand for sustainable materials and environmentally friendly processing technologies that can reduce energy consumption while minimizing ecological impacts [4], [5], [6]. In response to these challenges, renewable biomass-derived materials have emerged as promising alternatives due to their abundance, biodegradability, renewability, and lower environmental footprint compared with conventional synthetic materials [7], [8], [9].

The increasing global demand for sustainable and environmentally friendly materials has driven extensive research into cellulose-based materials derived from renewable resources [10], [11], [12]. Among these, bacterial cellulose (BC), a biopolymer produced by certain bacterial strains, has garnered significant attention due to its remarkable properties, including high mechanical strength, biocompatibility, and transparency. These characteristics make BC films highly suitable for diverse applications, such as packaging, flexible electronics, and biomedical devices [13], [14]. Unlike plant-based cellulose, BC is free from lignin and hemicellulose, allowing for the production of highly pure cellulose materials with a well-defined nanofiber network structure [15].

Despite these advantages, the practical use of BC films is often limited by their relatively modest thermal and mechanical properties [16]. Enhancing these properties is critical to expanding the application potential of BC films. Traditional methods of property enhancement, such as chemical modification and blending, often involve energy-intensive processes or hazardous chemicals, which contradict the goals of environmental sustainability. Consequently, there is a pressing need for eco-friendly and energy-efficient methods to improve the functional performance of BC films.

Ultrasonication has emerged as a promising green technique for modifying the structural and functional properties of cellulose materials. By applying high-frequency sound waves, ultrasonication can disrupt aggregates, improve dispersion, and alter the nanoscale morphology of cellulose fibers, potentially enhancing both the thermal and mechanical properties of BC films [17]. However, the effects of ultrasonication on BC films are highly dependent on processing parameters, such as the power and duration of sonication. Previous studies have successfully prepared cellulose films from BC powder sourced from pellicles [18]. Increasing the ultrasonic probe power enhanced transparency and mechanical properties, but reduced heat resistance. Prolonged ultrasonication may yield films with superior mechanical strength but could also compromise their thermal stability, leading to trade-offs that must be carefully managed [19], [20].

Despite the growing body of literature on ultrasonication in cellulose processing, a gap still exists in understanding the nuanced relationship between ultrasonication duration and BC films' properties. Specifically, the balance between thermal and mechanical properties needs further exploration. Addressing this gap is essential for optimizing BC films for high-performance applications. Our work aims to systematically investigate the influence of ultrasonication duration on the thermal and mechanical properties of BC films. The ultrasonication durations of 15 and 30 min were selected based on previous studies and preliminary observations indicating that this range is sufficient to improve cellulose fibril dispersion while minimizing excessive degradation of the cellulose structure [21]. These durations were chosen to represent moderate and extended ultrasonication treatments for evaluating the effect of sonication time on film properties. By analysing the effects of 15-minute and 30-minute sonication treatments, this work seeks to elucidate the trade-offs involved and provide a framework for optimizing BC film performance. The findings contribute to advancing sustainable material development by offering a simple and eco-friendly strategy for enhancing non-wood-based cellulose films.

## 2. Material and methods

### 2.1 Material

The original BC pellicle was obtained from a small-scale industry in Padang, Indonesia that originated in the form of nata de coco, a proprietary mixture of glucose, acetic acid, and coconut water with *Acetobacter xylinum*. 2,2,6,6-Tetramethylpiperidine-1-oxyl (TEMPO), sodium hypochlorite (NaClO), and sodium bromide (NaBr) were purchased from Sigma-Aldrich.

## 2.2 Preparation of TEMPO treated BC nanopaper

All Preparation of BC Suspension: BC powder (1 g, 200 mesh) was dispersed in 200 g of distilled water (0.5 wt%) containing 0.018 g TEMPO, 0.2 g NaBr, and 7.4 g NaClO. The mixture was stirred at 50 °C for 20 min using a magnetic stirrer to initiate TEMPO-mediated oxidation. Subsequently, 0.5 M NaOH was added to adjust the pH to 10, and the suspension was heated at 70 °C for 6 h. After cooling naturally for 12 h, the oxidized suspension was centrifuged at 3000 rpm for 30 min.

Preparation of BC powders and BC Films: The TOBC suspension was transferred to a glass tube for centrifugation using an LD-3 Electronic Centrifuge, operated at 3000 rpm for 30 minutes. Following centrifugation, the nanofiber precipitates were collected at the bottom of the tube. The water in the tube was replaced with fresh distilled water, and this washing process was repeated until the suspension achieved a neutral pH of 7. The resulting residue was processed with a high-shear homogenizer (WiseTis Homogenizer HG-15D, DAIHAN Scientific Co., Ltd., Gangwon-do, Korea) at 8000 rpm for 30 minutes. Ultrasonication was performed using an FS-1200N ultrasonic homogenizer (20 kHz, 1200 W) equipped with a 20 mm titanium alloy (Ti-6Al-4V) probe. The suspension was sonicated for 15 and 30 min, respectively.

Each sonicated BC suspension was subsequently heated at 100 °C on a magnetic stirrer for 4 hours. Once cooled to room temperature, the suspension was poured onto a Teflon plate (12 cm diameter) and dried in a Universal Oven Memmert UN-55 at 50 °C for 48 hours. The dried TOBC films were stored in a vacuum desiccator at 50% relative humidity (RH). The unsonicated sample was designated as U-0, while those sonicated for 15 and 30 minutes were labeled U-15 and U-30, respectively.

## 2.3 Morphological, optical, structural, thermal, and mechanical characterization

The surface morphology of the BC film samples was observed using field emission scanning electron microscopy (FESEM). Prior to analysis, the films were mounted on SEM stubs and sequentially coated with carbon and gold to minimize electron charging. FESEM observation was conducted using a JEOL JFIB 4610 instrument operated at an accelerating voltage of 15 kV and a probe current of 8 mA. Film opacity and optical properties were analyzed using a Shimadzu UV-1800 spectrophotometer (Japan). Rectangular film samples (1 × 2.5 cm) were scanned within the wavelength range of 200-800 nm according to ASTM D1003-00 for haze and luminous transmittance measurements of transparent plastics. Film opacity was determined from the area under the absorbance spectrum, and all measurements were performed in triplicate.

Fourier transform infrared spectroscopy (FTIR) analysis of non-sonicated and sonicated BC samples was carried out using a PerkinElmer Frontier spectrometer. Dried film samples were scanned over the wavenumber range of 4000-400 cm<sup>-1</sup> at a resolution of 4 cm<sup>-1</sup>. X-ray diffraction (XRD) analysis was performed using a PANalytical Xpert PRO diffractometer at 25 °C with an operating voltage of 40 kV and a current of 30 mA. The samples were scanned over a 2θ range of 3°-100°. The crystallinity index (CI) was calculated using Equation (1).

$$CI (\%) = \frac{(I_{200} - I_{am})}{I_{200}} \times 100 \quad (1)$$

where  $I_{200}$  represents the intensity of the crystalline peak corresponding to cellulose I, and  $I_{am}$  denotes the intensity of the amorphous region. Thermal resistance of the samples was evaluated using a Shimadzu DTG-60 thermal analysis instrument under a nitrogen flow rate of 50 mL/min. The temperature was increased at a heating rate of 20 °C/min. Tensile properties were measured

using a COM-TEN 95T Series 5K universal testing machine (Pinellas Park, USA) at room temperature with a crosshead speed of 5 mm/min according to ASTM D638 Type V. The toughness (TN) of the films was determined from the engineering stress–strain curves obtained during tensile testing. Toughness was calculated as the total area under the stress-strain curve up to the fracture point using the integration function in OriginPro software. The resulting values were expressed in MJ/m<sup>3</sup>, representing the energy absorbed per unit volume before failure.

Prior to testing, all samples were conditioned in a desiccator at 25 °C and 50% relative humidity for 48 h. Tensile measurements were repeated five times for each treatment. Statistical significance of the tensile property data was analyzed using analysis of variance (ANOVA), followed by Duncan’s multiple range test at a significance level of  $p \leq 0.05$ .

### 3. Results and discussion

#### 3.1 BC suspension and film appearance, and transmittance value

TEMPO treated BC suspension without (left side in Figure 1) and with ultrasonication (a center and the right position in Figure 1) present good nanofiber stability. After drying this suspension, each BC film had good transparency. The object under the film was still observable clearly. After testing the transmittance value of the dried film from 200-800 nm wavelength, the transparency increased with increasing ultrasonic duration (Figure 1e). Ultrasonication treatment for 15 and 30 min shifts of the light transmittance at 650 nm from 33.9% to 39.5% (U-15 film) and 42.3% (U-30 film), respectively (Table 1). The 30 min sonicated film was the most transparent due to the lowest light reflection passing through the film. The increased transparency is because the size of the nanofibrils is much less than the wavelength of visible light, thus highly transparent with a significant light scattering in the forward direction [22]. This finding is consistent with Figure 2, showing more compact fiber structures and finer diameters after ultrasonication. The higher transparency is also associated with an increase in the crystal index of the film, as shown in Figure 3, presenting a higher CI value of U-30 film (84.1%) than U-0 film (82.0%) (Table 1). The highly crystalline film consisting of densely packed cellulose molecules reflects light small enough [23][24].

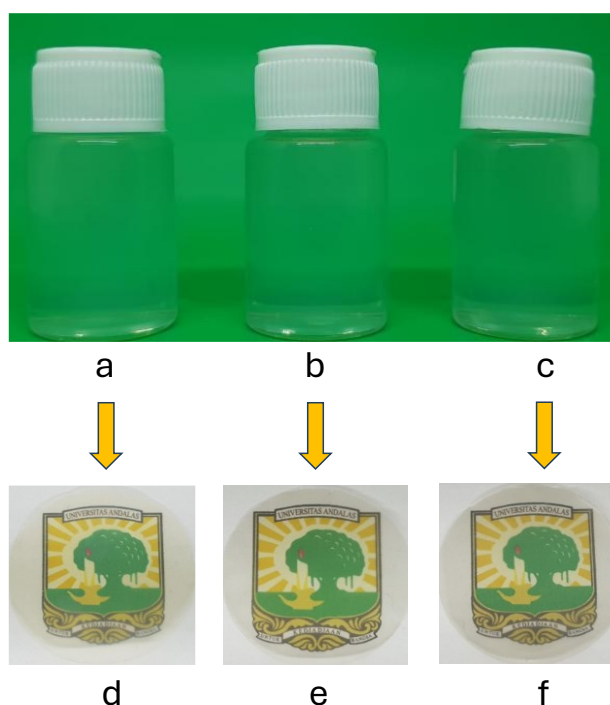


**Figure 1.** Suspension and transparent film of non-sonicated-BC (a, d), sonicated-BC for 15 min (b, e), and 30 min (c, g)

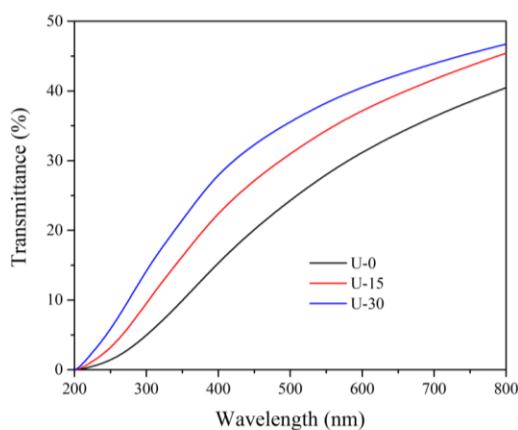


**Figure 2.** U-0 film, c) U-15 film, d) U-30 film, and e) transmittance curve of films

### 3.2 FESEM morphology

Figure 3 displays the FESEM morphology of the surface of the tensile specimens without and with ultrasonication treatment. The non-sonicated sample (Figure 3a) contains a large-sized hollow (orange arrow), randomly distributed BC nanofibers, and a sparse nanofiber configuration confirming a non-compacted structure. The presence of these defects led to a more brittle BC film. After ultrasonication, BC nanofibers were increasingly oriented, fiber density became higher, the number of big hollows decreased, and neatly arranged layers of BC nanofiber became more evident (Figures 3b and 3c). This result led to a larger surface contact area of sonicated BC nanofibers than non-sonicated ones. More contact surface enable an increase in cross-linking hydrogen bonds between polymer chains.

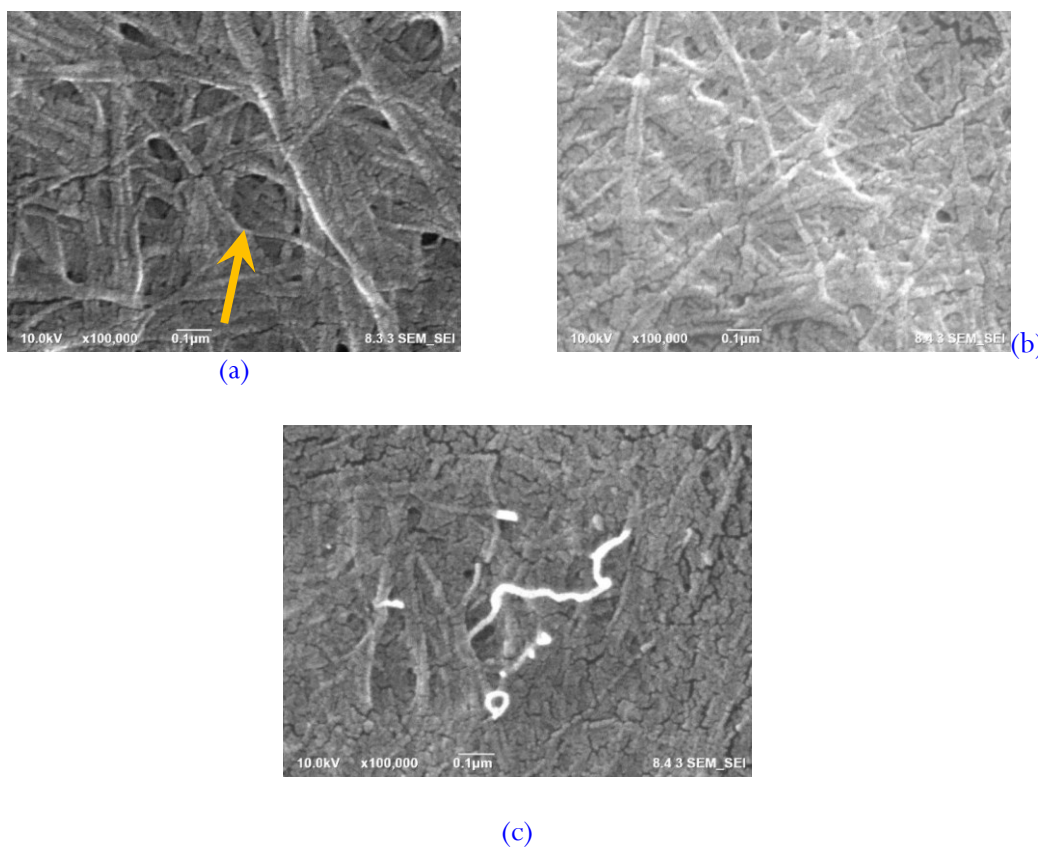


**Figure 3.** FE-SEM surface morphology of the films without ((a) U-0) and with ultrasonication treatment ((b) U-15 and (c) U-30 film). The film thickness was about 50 microns

### 3.3 FTIR spectra

FTIR spectroscopy can be used to characterize the functional groups of cellulose [25]. Figure 4 shows the FTIR spectra for BC films treated without and with different ultrasonication duration of 15 min and 30 min. The FTIR pattern of all films is broadly similar, indicating that ultrasonication treatment did not significantly affect the chemical structure of BC. A similar finding agrees with previous works [26][27]. The broad absorption band observed at approximately 3337-3338  $\text{cm}^{-1}$  corresponds to O-H stretching vibrations, while the bands around 2890  $\text{cm}^{-1}$  and 1030-1160  $\text{cm}^{-1}$  are associated with C-H stretching and C-O-C/C-O vibrations of the cellulose backbone, respectively. Although minor variations in peak position and intensity were observed among the samples, these differences were relatively small and may fall within instrumental uncertainty. Therefore, no substantial chemical changes can be inferred from the FTIR spectra. The results suggest that ultrasonication mainly influenced the physical arrangement and dispersion of cellulose fibrils rather than the chemical composition of the cellulose structure.

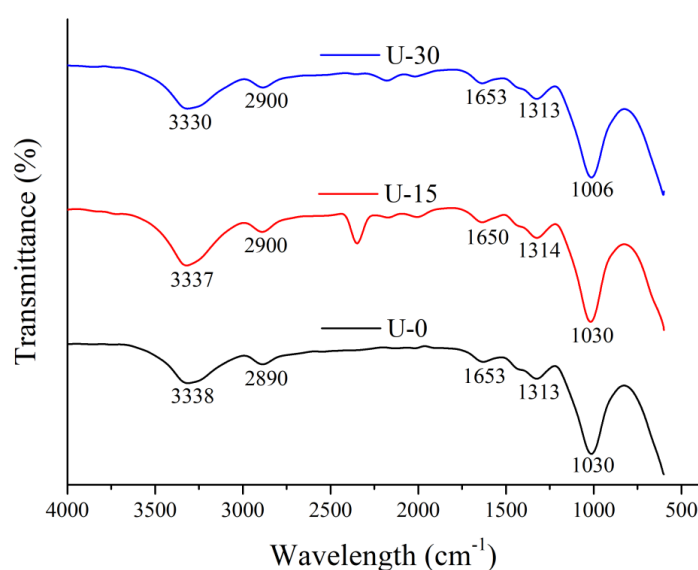


**Figure 4.** FTIR patterns for U-0 (black), U-15 (red), and U-30 film (blue)

### 3.4 XRD

Figure 5 shows the X-ray diffraction pattern of BC without and with ultrasonication treatment. All non- and sonicated BC films have typical cellulose I diffraction patterns with two main peaks at  $2\theta = 22$  and  $14^\circ$ . This result agrees with the previously reported diffraction pattern [28]. Ultrasonication treatment of non-sonicated BC for 30 min increased CI value from 82.02% to 84.14% due to the reduction of amorphous regions [28]. This decrement is because the kinetic energy of a liquid jet destroyed firstly amorphous sections due to lower resistance against sonication attacks than crystalline domains [29], [30]. After ultrasonication, the  $2q$  value increased, and the  $d$ -spacing of the (200) plane decreased (Table 1). These shifts express the sonicated BC film bear higher compressive residual stress [31], [32]. It confirms that sonicated BC films demonstrate a more compact chain structure than non-sonicated. Consequently, the cellulose chains become more difficult to slippage [33], [34]. Although a slight increase in crystallinity was observed after ultrasonication, the enhanced transparency is primarily attributed to improved fibril dispersion and the reduction of structural heterogeneities that scatter visible light. Ultrasonication promotes a more uniform and compact cellulose network, thereby facilitating light transmission through the film. The increase in crystallinity may further contribute to structural ordering; however, it is unlikely to be the dominant factor governing transparency.

**Table 1.** The crystallinity index (CI) for different treated BC films

Samples	Transmittance (%) at 650 nm	CI (%) of (200) plane	2 $\theta$ of (200) plane	d-spacing [Å] of (200) plane	T <sub>max</sub> (°C)	Latent heat of fusion (kJ/g)
U-0	33.9	82.02	20.64	4.30	317.2	0.03
U-15	39.5	82.07	22.98	3.87	351.1	1.22
U-30	42.3	84.14	22.71	3.91	322.6	1.04

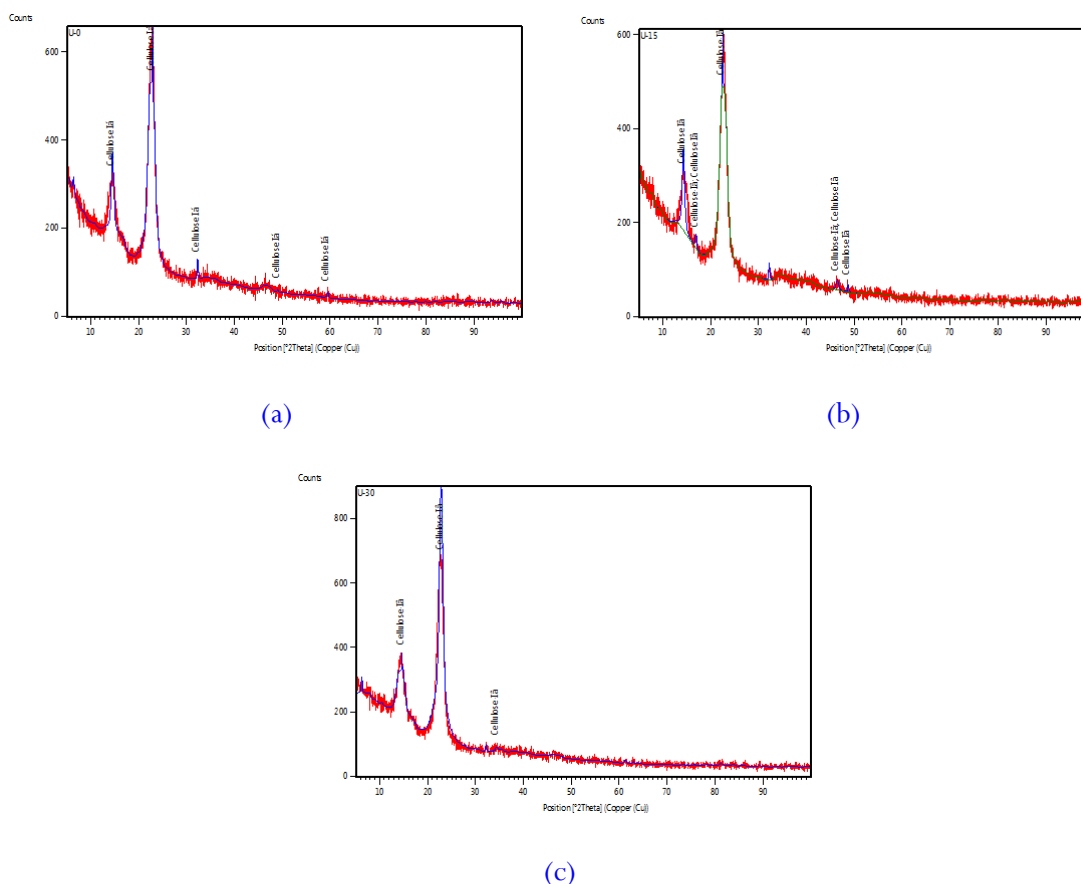


**Figure 5.** X-ray diffraction patterns of (a) U-0, (b) U-15, and (c) U-30 film

### 3.5 Thermal properties

Figure 6(a and b) displays the thermal properties of BC without and with ultrasonication. The first weight losses of all BC samples (60-150 °C) were due to evaporation of absorbed water [35]. The samples present various weight losses because of the different amounts of water evaporated. In the second step in the range 300-420 °C, a considerable weight loss is associated with the decomposition of cellulose [36]. The sonicated BC film had higher thermal resistance than non-sonicated BC. This phenomenon can be observed at the maximum decomposition temperature (T<sub>max</sub>) and the weight loss percentage. The T<sub>max</sub> for the U-0 sample was 317.2 °C, shifted to 351.1 °C after ultrasonication for 15 min (U-15 film). The latent heat of fusion of U-0 film was 0.03 kJ/g, also lower than that of U-15 film (1.22 kJ/g). The U-0 sample lost 59.6% of its weight higher than the U-15 film (59.4%) and U-30 film (52.3%). The higher T<sub>max</sub> observed for the sonicated samples indicates an improvement in thermal resistance compared with the untreated film. This behavior suggests that ultrasonication modified the cellulose microstructure, resulting in delayed thermal degradation. The improved thermal stability of U-15 may be attributed to enhanced fibril dispersion and stronger

intermolecular hydrogen bonding resulting from ultrasonication. However, prolonged ultrasonication (U-30) may induce partial cellulose chain scission due to intense cavitation effects. Consequently, although the crystallinity index remained high, degradation of cellulose chains may offset the beneficial effect of increased crystallinity on thermal stability. This tendency agrees with previous works [37]. Finally, a third weight loss is present over 420 °C due to the decomposition of charcoal.

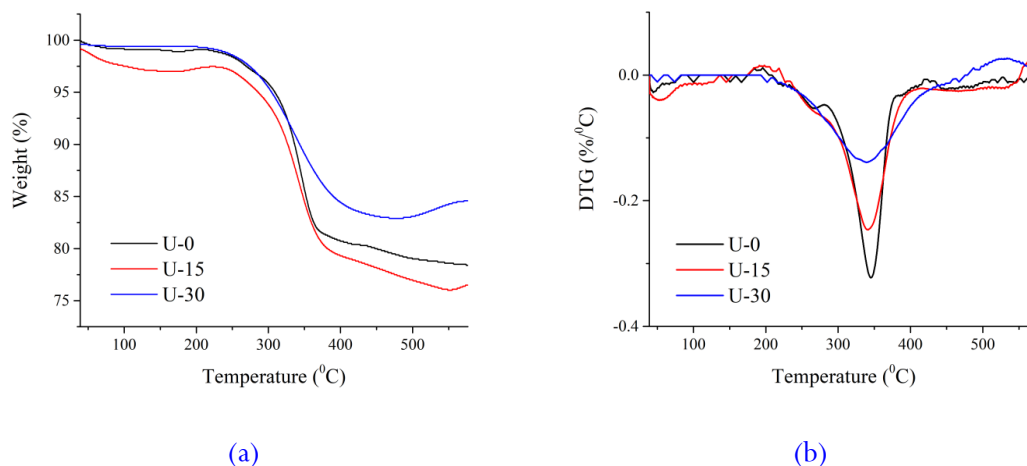


**Figure 6.** a) TGA, and b) DTA curve for non- and sonicated BC film

### 3.6 Tensile properties

Figure 7a shows a uniaxial stress-strain curve of the samples. The U-0 film presents the lowest stress-strain value. Figures 6b, 6c, 6d, and 6e show the average value of tensile strength (TS), tensile modulus (TM), elongation at break (EB), and toughness (TN), respectively, for all films. The TS, EB, and TN values for the U-0 film were 46.41 MPa, 5.79%, and 1.72 MJ/m<sup>3</sup>. After more prolonged sonication treatment, the TS, TM, and TN values increased, but EB remained constant. The ultrasonication duration of 30 min increased TS by 165.78% (123.36 MPa), TM 294.79% (4226.93 MPa), EB 19.3% (4.67%), and TN 119.77% (3.78 MJ/m<sup>3</sup>), compared to the U-0 film. These increased tensile properties correspond to more compacted cellulose structures and higher contacted nanofiber density [38]. Higher interconnected nanofibers of the sonicated film led to increased hydrogen bonding between cellulose chains [39]. Surprisingly, although the film's tensile strength increases, the EB value does not decrease relatively. This phenomenon may be caused by the lower energy required for the slippage of strongly interlinked cellulose chains than for crack propagation through the film [40], [41].

This finding is consistent with the FTIR pattern showing stronger hydrogen-hydrogen interconnection (Figure 4) and FESEM higher cellulose chain compatibility (Figure 2b) as increasing ultrasonication duration. Furthermore, the simultaneous enhancement of TS, TM, and TN demonstrates that ultrasonication improves stress transfer throughout the cellulose network without compromising deformation capability. While increased stiffness is often associated with reduced toughness, the sonicated films maintained their ability to absorb deformation energy before failure. This behavior suggests that ultrasonication promotes a more homogeneous fiber distribution and stronger interfibrillar interactions, resulting in a denser nanofibrillar network. The substantial increase in tensile modulus indicates the formation of a rigid cellulose structure with enhanced load-bearing capability. During ultrasonication, the disruption of weakly bonded fiber aggregates may expose additional cellulose surfaces, increasing nanofiber contact and promoting intermolecular hydrogen bonding. This interpretation is supported by the FTIR and SEM results, which indicate stronger intermolecular interactions and a more compact morphology.

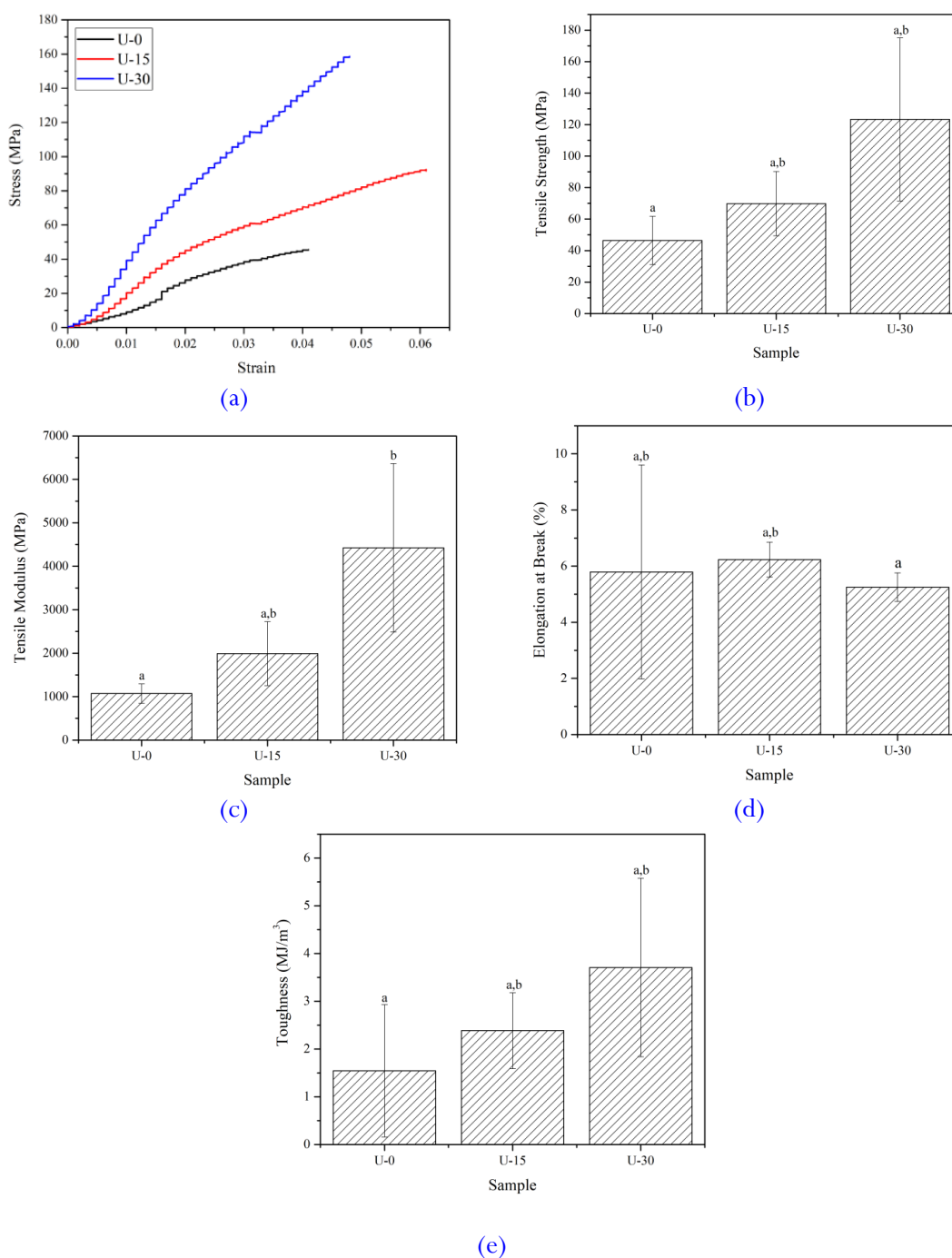


**Figure 7.** Stress-strain curve for all treated films (a). Average values of TS (b), TM (c), EB (d), and TN (e) for non- and sonicated film. Different letters for each data point explain a significant difference in mean values ( $p \leq 0.05$ ). The same letter indicates values are not significantly different

#### 4. Conclusion

This study investigated the effect of ultrasonication duration on the structural, optical, thermal, and mechanical properties of bacterial cellulose films prepared from BC powder. The results demonstrated that ultrasonication effectively improved fibril dispersion and promoted a more homogeneous film structure, leading to enhanced transparency, tensile strength, and toughness. The findings also revealed that the influence of ultrasonication on thermal behavior differed from its effect on mechanical performance, highlighting the existence of trade-offs among the resulting properties. Overall, the study demonstrates that ultrasonication is a simple, environmentally

friendly, and effective processing strategy for tailoring the performance of bacterial cellulose films. These findings provide useful guidance for the development of sustainable cellulose-based materials for advanced engineering and packaging applications.

### Author's declaration

### Author contribution

**Dieter Rahmadiawan:** Formal analysis, validation, writing-original draft, and writing-review and editing. **Tio Baskara:** Investigation, visualization, and writing-original draft. **Hairul Abral:** Supervision, conceptualization, methodology, project administration, resources, and writing-review and editing. **Eni Sugiarti:** Resources. **Ahmad Novi Muslimin:** Investigation. **Shih-Chen Shi:** Validation, writing-review and editing. **Thiago F. Santos:** Validation, Writing-review and editing. **Imtiaz Ali Laghari:** Formal analysis, writing-review and editing.

### Funding statement

Not applicable.

### Data availability

The data supporting the findings of this study are available from the corresponding author upon reasonable request.

### Acknowledgements

Not applicable.

### Competing interest

The authors declare that they are NOT affiliated with or involved in any organization or entity that has a financial interest (such as honoraria; educational grants; participation in speakers' bureaus; membership, employment, consulting, stock ownership, or other equity interests; and expert testimony or patent licensing arrangements), or non-financial interest (such as personal or professional relationships, affiliations, knowledge, or beliefs) in the subject matter or materials discussed in this manuscript.

### Ethical clearance

Not applicable.

### AI statement

The grammatical structure of this article was improved by using ChatGPT and the authors have rechecked the accuracy and correctness of the generated sentences with the topic and data of this study. The language use in this article has been validated and verified by an English language expert and none of the AI-generated sentences include in this article.

### Publisher's and Journal's note

Universitas Negeri Padang as the publisher, and Editor of Teknomekanik state that there is no conflict of interest towards this article publication.

## References

- [1] I. A. Laghari *et al.*, “Thermal energy harvesting of highly conductive graphene-enhanced paraffin phase change material,” *Journal of Thermal Analysis and Calorimetry* 2023 148:18, vol. 148, no. 18, pp. 9391–9402, Aug. 2023, <https://doi.org/10.1007/S10973-023-12336-5>
- [2] M. A. Koonthar, I. A. Laghari, B. M. Asfaw, R. Reji Kumar, and A. H. Lenin, “Experimental and simulation-based comparative analysis of different parameters of PV module,” *Sci. Afr.*, vol. 16, p. e01197, Jul. 2022, <https://doi.org/10.1016/J.SCIAF.2022.E01197>
- [3] I. A. Laghari, M. Samykan, A. K. Pandey, K. Kadirgama, and Y. N. Mishra, “Binary composite (TiO<sub>2</sub>-Gr) based nano-enhanced organic phase change material: Effect on thermophysical properties,” *J. Energy Storage*, vol. 51, p. 104526, Jul. 2022, <https://doi.org/10.1016/J.EST.2022.104526>
- [4] A. Setiawan, P. Puspitasari, M. Tauviquirrahman, D. D. Pramono, and H. Salam, “Performance analysis of soybean oil with CuO/Graphene hybrid additive nanoparticles as cutting fluid on CNC machining processes,” *Teknomekanik*, vol. 8, no. 2, pp. 136–163, Nov. 2025, <https://doi.org/10.24036/Teknomekanik.V8I2.42472>
- [5] D. Rahmadiawan, N. Aslfattahi, N. Nasruddin, R. Saidur, A. Arifutzzaman, and H. A. Mohammed, “MXene Based Palm Oil Methyl Ester as an Effective Heat Transfer Fluid,” *Journal of Nano Research*, vol. 68, pp. 17–34, 2021, <https://doi.org/10.4028/www.scientific.net/JNANOR.68.17>
- [6] D. Rahmadiawan, H. Abral, N. Nasruddin, and Z. Fuadi, “Stability, Viscosity, and Tribology Properties of Polyol Ester Oil-Based Biolubricant Filled with TEMPO-Oxidized Bacterial Cellulose Nanofiber,” *Int. J. Polym. Sci.*, vol. 2021, no. 1, p. 5536047, Jan. 2021, <https://doi.org/10.1155/2021/5536047>
- [7] I. A. Laghari, M. Samykan, A. K. Pandey, K. Kadirgama, and V. V. Tyagi, “Advancements in PV-thermal systems with and without phase change materials as a sustainable energy solution: energy, exergy and exergoeconomic (3E) analytic approach,” *Sustain. Energy Fuels*, vol. 4, no. 10, pp. 4956–4987, Sep. 2020, <https://doi.org/10.1039/D0SE00681E>
- [8] A. Amri *et al.*, “The conversion of nata de coco bacterial cellulose into cellulose nanofibers using high shear mixer with eco-friendly fluid dynamics method,” *Teknomekanik*, vol. 7, no. 2, pp. 139–155, Dec. 2024, <https://doi.org/10.24036/TEKNOMEKANIK.V7I2.32972>
- [9] D. Rahmadiawan *et al.*, “Enhanced durability and tribological performance of polyvinyl alcohol/layered double hydroxide/tannic acid composites under repeated swelling cycles,” *Teknomekanik*, vol. 7, no. 2, pp. 101–111, Dec. 2024, <https://doi.org/10.24036/Teknomekanik.V7I2.32872>
- [10] T.-T. Huang, D. Rahmadiawan, and S.-C. Shi, “Synthesis and characterization of porous silica and composite films for enhanced CO<sub>2</sub> adsorption: A circular economy approach,” *Journal of Materials Research and Technology*, vol. 32, pp. 1460–1468, 2024, <https://doi.org/https://doi.org/10.1016/j.jmrt.2024.08.003>
- [11] Kadriadi *et al.*, “A novel active packaging film based on PVAbajakah tampala (*Spatholobus littoralis* hassk) extract: Enhancing mechanical, UV protection, thermal stability, antimicrobial, and barrier properties,” *Food Biosci.*, vol. 68, p. 106500, 2025, <https://doi.org/https://doi.org/10.1016/j.fbio.2025.106500>
- [12] D. Rahmadiawan, S. C. Shi, N. Aslfattahi, A. N. Fauza, and Z. Fuadi, “Advancements in Cellulose for Eco-Friendly Lubricant Applications: A Review on Tribological Properties,” *ACS Omega*, vol. 10, no. 33, pp. 36878–36889, Aug. 2025, <https://doi.org/10.1021/acsomega.5c05037>
- [13] D. Klemm *et al.*, “Nanocellulose as a natural source for groundbreaking applications in materials science: Today’s state,” *Materials Today*, vol. 21, no. 7, pp. 720–748, 2018, <https://doi.org/10.1016/j.mattod.2018.02.001>

- [14] T. C. de Souza *et al.*, “Magnetic Bacterial Cellulose Biopolymers: Production and Potential Applications in the Electronics Sector,” *Polymers (Basel)*, vol. 15, no. 4, pp. 1–15, 2023, <https://doi.org/10.3390/polym15040853>
- [15] A. K. Saleh, H. El-Gendi, G. A. G. Ammar, and T. H. Taha, “Sustainable production of bacterial cellulose from delignified rice straw using *Novacetimonas hansenii* TGA isolate: Process optimization and membrane characterization,” *Int. J. Biol. Macromol.*, vol. 320, p. 146136, 2025, <https://doi.org/10.1016/j.ijbiomac.2025.146136>
- [16] X. Hu *et al.*, “A bacterial cellulose composite separator with high thermal stability and flame retardancy for high-performance lithium ion batteries,” *J. Colloid Interface Sci.*, vol. 679, pp. 633–642, 2025, <https://doi.org/10.1016/j.jcis.2024.10.123>
- [17] B. Zakani, S. Entezami, D. Grecov, H. Salem, and A. Sedaghat, “Effect of ultrasonication on lubrication performance of cellulose nano-crystalline (CNC) suspensions as green lubricants,” *Carbohydr. Polym.*, vol. 282, no. May 2021, p. 119084, 2022, <https://doi.org/10.1016/j.carbpol.2021.119084>
- [18] D. Rahmadiawan *et al.*, “A Novel Highly Conductive, Transparent, and Strong Pure-Cellulose Film from TEMPO-Oxidized Bacterial Cellulose by Increasing Sonication Power,” *Polymers (Basel)*, vol. 15, no. 3, p. 643, 2023, <https://doi.org/10.3390/polym15030643>
- [19] S. Coseri *et al.*, “One-shot carboxylation of microcrystalline cellulose in the presence of nitroxyl radicals and sodium periodate,” *RSC Adv.*, vol. 5, no. 104, pp. 85889–85897, 2015, <https://doi.org/10.1039/c5ra16183e>
- [20] R. K. Gupta, U. Gnana Moorthy Eswaran, S. Kumar, S. Pipliya, B. Kaur, and P. P. Srivastav, “Synergistic Modification of Starch Polysaccharide via Sequential Treatments With Ultrasonic and Cold Plasma Technology,” *J. Food Process. Preserv.*, vol. 2025, no. 1, p. 9063007, Jan. 2025, <https://doi.org/10.1155/jfpp/9063007>
- [21] N. Thirunavookarasu, S. Kumar, P. Shetty, A. Shanmugam, and A. Rawson, “Impact of ultrasound treatment on the structural modifications and functionality of carbohydrates – A review,” *Carbohydr. Res.*, vol. 535, p. 109017, 2024, <https://doi.org/10.1016/j.carres.2023.109017>
- [22] L. Hu *et al.*, “Transparent and conductive paper from nanocellulose fibers,” *Energy Environ. Sci.*, vol. 6, no. 2, pp. 513–518, 2013, <https://doi.org/10.1039/c2ee23635d>
- [23] H. Abrial *et al.*, “Transparent and antimicrobial cellulose film from ginger nanofiber,” *Food Hydrocoll.*, vol. 98, p. 105266, 2020, <https://doi.org/10.1016/j.foodhyd.2019.105266>
- [24] M. Nogi, S. Iwamoto, A. N. Nakagaito, and H. Yano, “Optically Transparent Nanofiber Paper,” *Advanced Materials*, vol. 21, no. 16, pp. 1595–1598, 2009, <https://doi.org/10.1002/adma.200803174>
- [25] R. A. Ilyas, S. M. Sapuan, and M. R. Ishak, “Isolation and characterization of nanocrystalline cellulose from sugar palm fibres (*Arenga Pinnata*),” *Carbohydr. Polym.*, vol. 181, pp. 1038–1051, 2018.
- [26] R. Zhang, Y. Wang, D. Ma, S. Ahmed, W. Qin, and Y. Liu, “Effects of ultrasonication duration and graphene oxide and nano-zinc oxide contents on the properties of polyvinyl alcohol nanocomposites,” *Ultrason. Sonochem.*, vol. 59, no. August, p. 104731, 2019, <https://doi.org/10.1016/j.ultsonch.2019.104731>
- [27] H. Abrial, V. Lawrensius, D. Handayani, and E. Sugiarti, “Preparation of nano-sized particles from bacterial cellulose using ultrasonication and their characterization,” *Carbohydr. Polym.*, vol. 191, pp. 161–167, 2018, <https://doi.org/10.1016/j.carbpol.2018.03.026>
- [28] Q. Lu *et al.*, “Preparation and characterization of cellulose nanocrystals via ultrasonication-assisted FeCl<sub>3</sub>-catalyzed hydrolysis,” *Cellulose*, vol. 21, no. 5, pp. 3497–3506, 2014, <https://doi.org/10.1007/s10570-014-0376-2>



- [29] E. Y. Wardhono, N. Kanani, and A. Alfirano, "A simple process of isolation microcrystalline cellulose using ultrasonic irradiation," *J. Dispers. Sci. Technol.*, vol. 41, no. 8, pp. 1217–1226, 2020, <https://doi.org/10.1080/01932691.2019.1614947>
- [30] R. Qu, M. Tang, Y. Wang, D. Li, and L. Wang, "TEMPO-oxidized cellulose fibers from wheat straw: Effect of ultrasonic pretreatment and concentration on structure and rheological properties of suspensions," *Carbohydr. Polym.*, vol. 255, no. November 2020, p. 117386, 2021, <https://doi.org/10.1016/j.carbpol.2020.117386>
- [31] H. Abrial *et al.*, "Characterization of compressed bacterial cellulose nanopaper film after exposure to dry and humid conditions," *Journal of Materials Research and Technology*, vol. 11, pp. 896–904, 2021, <https://doi.org/10.1016/j.jmrt.2021.01.057>
- [32] J. Epp, *X-Ray Diffraction (XRD) Techniques for Materials Characterization*. Elsevier Ltd, 2016. <https://doi.org/10.1016/B978-0-08-100040-3.00004-3>
- [33] A. Izumi, T. Kakara, M. W. Otsuki, Y. Shudo, T. Koganezawa, and M. Shibayama, "In situ residual stress analysis in a phenolic resin and copper composite material during curing," *Polymer (Guildf)*, vol. 182, no. October, p. 121857, 2019, <https://doi.org/10.1016/j.polymer.2019.121857>
- [34] Q. Meng and T. J. Wang, "Mechanics of Strong and Tough Cellulose Nanopaper," *Appl. Mech. Rev.*, vol. 71, no. 4, pp. 040801–30, 2019, <https://doi.org/10.1115/1.4044018>
- [35] M. Asrofi, H. Abrial, Y. Kurnia, S. M. Sapuan, and H. Kim, "Effect of duration of sonication during gelatinization on properties of tapioca starch water hyacinth fiber biocomposite," *Int. J. Biol. Macromol.*, vol. 108, pp. 167–176, 2018.
- [36] C. N. Wu and K. C. Cheng, "Strong, thermal-stable, flexible, and transparent films by self-assembled TEMPO-oxidized bacterial cellulose nanofibers," *Cellulose*, vol. 24, no. 1, pp. 269–283, 2017, <https://doi.org/10.1007/s10570-016-1114-8>
- [37] H. Yousefi, M. Faezipour, S. Hedjazi, M. M. Mousavi, Y. Azusa, and A. H. Heidari, "Comparative study of paper and nanopaper properties prepared from bacterial cellulose nanofibers and fibers/ground cellulose nanofibers of canola straw," *Ind. Crops Prod.*, vol. 43, no. 1, pp. 732–737, 2013, <https://doi.org/10.1016/j.indcrop.2012.08.030>
- [38] S. Wang *et al.*, "Transparent, Anisotropic Biofilm with Aligned Bacterial Cellulose Nanofibers," *Adv. Funct. Mater.*, vol. 28, no. 24, pp. 1–10, 2018, <https://doi.org/10.1002/adfm.201707491>
- [39] I. A. Udoetok, L. D. Wilson, and J. V. Headley, "Ultra-sonication assisted cross-linking of cellulose polymers," *Ultrason. Sonochem.*, vol. 42, no. October 2017, pp. 567–576, 2018, <https://doi.org/10.1016/j.ultsonch.2017.12.017>
- [40] J. A. da Cruz *et al.*, "Poly(vinyl alcohol)/cationic tannin blend films with antioxidant and antimicrobial activities," *Materials Science and Engineering C*, vol. 107, no. October 2019, p. 110357, 2020, <https://doi.org/10.1016/j.msec.2019.110357>
- [41] A. Celzard, W. Zhao, A. Pizzi, and V. Fierro, "Mechanical properties of tannin-based rigid foams undergoing compression," *Materials Science and Engineering A*, vol. 527, no. 16–17, pp. 4438–4446, 2010, <https://doi.org/10.1016/j.msea.2010.03.091>